

# Urban Heat Island Amplification Estimates on Global Warming Using an Albedo Model

Alec Feinberg

**Key Words:** Urban Heat Islands, Albedo Modeling, UHI Amplification Effects, Global Warming Causes and Amplification Effects, UHI Footprint, UHI Heat Dome, Cool Roofs, Sea Ice and Moisture Feedbacks

**Abstract** In this paper we provide nominal and worst case estimates of radiative forcing due to UHI effect (including urban areas) using a Weighted Amplification Albedo Solar Urbanization (WAASU) Model. This is done with the aid of reported findings from UHI footprint and heat dome studies that simplified estimates for UHI amplification factors. Using this method, we find between 1.6 and 7.5% of global warming may be due to the UHI effect (with urban areas). These values may increase to between 5 and 24% when rough climate feedbacks values are estimated. The model also found that the effect was proportional to the UHI amplification area coverage with an area sensitive estimate of about  $0.095 \text{ (W/m}^2\text{)/}\%$ Normalized Area. This value perhaps increases to  $0.3 \text{ W/m}^2\text{/}\%$ Normalized Area when rough climate feedbacks values are considered. The model is additionally used to quantify an assessment of sea ice feedback warming. Results provide insight into the UHI area effects from a new perspective and illustrates that one needs to take into account effective UHI amplification factors when assessing UHI's warming effect on a global scale. Lastly, such effects likely show a persuasive argument for the need of world-wide UHI albedo goals.

## 1 Introduction

It is concerning that there are so few UHI publications recently on their possible influences to global warming. Part of the motivation for this paper is to illustrate the continual need for more up-to-date related studies including UHI amplification effects (that include their urban areas) as will be discussed in this paper. The subject of UHI effect having significant contributions to global warming is very important and should remain so. The topic has a controversial history. One such paper, McKittrick and Michaels (2007) found that the net warming bias at the global level may explain as much as half the observed land-based warming. This study was criticized by Schmidt (2009) and defended for a period of about 10 years by McKittrick (see McKittrick Website). Other authors have also found significance (Zhao, 1991; Feddema et al., 2005; Ren et al., 2007, 2008; Jones et al., 2008; Stone, 2009; Zhao, 2011; Yang et al. 2011, and Haung et al. 2015). These studies used land-based temperature station data to make assessments. Although the studies have all found global warming UHI significance with different assessments, they have yet to influence the IPCC enough to necessitate albedo recommendations in their many reports and meetings like the CO<sub>2</sub> effort. This is important because we feel the IPCC's should be more proactive in helping the global community recognizing the need for UHI albedo guidelines. Although the IPCC have provided reports on UHIs including health related issues, the response to their reports does not appear to be effective on the global scale compared with the on-going CO<sub>2</sub> effort.

The contention that UHI effects are basically only of local significance is most likely related to urban area estimates. For example, IPCC (Satterthwaite et. al. 2014) AR5 report references Schneider et al. (2009) study that resulted in urban coverage of 0.148% of the Earth (Table 1). This seemingly small area tends to dismiss the contention that UHI effect can play a large scale role in global warming. Furthermore, estimates of how much of land has been urbanized vary widely in the literature and this is in part due to the definition of what is urban and the datasets used. Although, such estimates are important for environmental studies, obtaining true estimates for the small urbanized area relative to the total land is apparently very difficult. This is compounded by the fact that there is a significant difference in how groups define the term 'urban'. Thus, urbanized surface area land approximations vary widely and most are obtained with satellite measurements sometimes supplemented in some way with census data. Table 1 captures the variations from some papers that are of interest.

**Table 1.** Urbanization area extent estimates from various sources

Percent of Land	Percent of Earth	References
2.7	0.783	GRUMP, 2005 - using NASA satellite light studies based on 2004 data and supplemented with census data
1%	0.29	NASA, 2000; Galka, 2016 – from satellite data
0.51	0.148	Schneider et al. 2009 - based on 2000-2001 data and referenced in the IPCC report (Satterthwaite, 2014)
0.5%	0.145	Zhou 2015 - based on a 2000 data set

56  
57  
58  
59  
60  
61  
62  
63  
64  
65  
66  
67  
68  
69  
70  
71  
72  
73  
74  
75  
76  
77  
78  
79  
80  
81  
82  
83  
84  
85  
86  
87  
88  
89  
90  
91  
92  
93  
94  
95  
96  
97  
98  
99  
100  
101  
102  
103  
104  
105  
106  
107

In addition, global warming UHI amplification effects have not been quantified to a large degree related to area estimates. Urbanized average solar areas remain unknown.

In our study, one key paper listed in the Table 1 is due to Schneider et al. (2009) since it is cited by the AR5 2014 IPCC report (Satterthwaite et al. 2014). In Schneider's paper, the larger area found in the GRUMP 2005 study (Table 1) is criticized. These area estimates are of interest in our paper for the *Weighted Amplification Albedo Solar Urbanization (WAASU) Model*. As well, the Amplification factors we use are related to their urban coverage estimates. In this paper we use both the Schneider et al. and GRUMP studies for the nominal and worst cases urbanization area estimates respectively. Furthermore, they were both done using data sets from around 2000 which is a convenient time to extrapolate down to 1950 and up to 2019 (see Sec. 3).

In our study, where we introduce the WAASU model, we will see that it has some advantages over the ground-based temperature studies like McKittricks and Michaels. The model is non probabilistic, in line with the way typical energy budgets are calculated. It uses only two key parameters (effective normalized area and average albedo). Because it is simplistic, it has transparency compared with the complex land-based studies.

### 1.1 UHI Amplification Effects

The table below lists the global warming causes and amplification effects. In this section we will summarize only the UHI amplification effects listed in the table since the root causes and the main global warming feedback amplification effects are fairly well known.

**Table 2.** Global warming cause and effects

<b>Global Warming Causes →</b>	Population → Expanding Urban Heat Islands (UHI), Roads & Increases in Greenhouse Gas
<b>Global Warming Feedback Amplification Effects →</b>	Water Vapor Feedback, Land Albedo Change Due to Cities & Roads, Ice and Snow –Albedo Feedback, Lapse Rate Feedback, Cloud Feedback, etc.
<b>Urban Heat Island Amplification Effects →</b>	UHI Solar Heating Area (Building Areas), UHI Building Heat Capacities, Humidity Effects and Hydro-Hotspots, Reduced Wind Cooling, Solar Canyons, Loss of Wetlands, Increase in Impermeable Surfaces, Loss of Evapotranspiration Natural Cooling.

The UHI amplification effects that we consider to dominate listed in the table are as follows:

- **The humidity amplification effect:** This has been observed. For example, Zhao et al. (2014) noted that UHI temperature increases in daytime  $\Delta T$  by  $3.0^{\circ}\text{C}$  in humid climates but decreasing  $\Delta T$  by  $1.5^{\circ}\text{C}$  in dry climates. They noted that such relationships imply that UHIs will exacerbate heat wave stress on human health in wet UHI climates. One explanation for this is how heat dissipates through convection which is more difficult in humid climates. Another explanation is that warmer air holds more water vapor. This can increase local specific humidity so that there could be local greenhouse effects.
- **The heat capacity and solar heating area amplification effect:** This contributes to the day-night UHI cycle. Here in most cities, it is observed that daytime atmospheric temperatures are actually cooler compared to night. For example, in a study by Basara et al. (2008) in Oklahoma city UHI it was found that at just 9-m height, the UHI was consistently  $0.5\text{--}1.75^{\circ}\text{C}$  greater in the urban core than the surrounding rural locations at night. Further, in general UHI impact was strongest during the overnight hours and weakest during the day. This inversion effect can be the results of massive UHI buildings acting like heat sinks, having giant heat capacities and storing heat in their reservoir via convection as solar radiation is absorbed during the day. This often reduces the UHI day effect, but at night buildings cools down, giving off their stored heat that increases local temperatures to the surrounding atmosphere. This effect increases with city growth as buildings have gotten substantially taller (Barr 2019) since 1950.
- **The hydro-hotspot amplification effect:** This effect is not well addressed. Here atmospheric moisture source is a complex issue due to Hydro HotSpots (HHS). Hydro hotspots occur when buildings are hot due to sun exposure. Then during precipitation periods, the hot highly evaporation surfaces increase localized water vapor in the air via the effect that warm air holds more moisture. This increase in local greenhouse gas, could blanket city heat and increase infrared radiation during these periods. This, as discussed above, is another possible UHI humidity amplification.

- 108 • **Reduced wind cooling and solar canyons:** In UHIs reduced wind is a known effect due to building wind  
 109 friction which inhibits cooling by convection. As well, tall buildings create solar canyons and trap sunlight  
 110 reducing the average albedo although some benefits occurs from shading. In general, both have the effect  
 111 of amplifying the temperature profile of UHIs.

## 112 2 Data and Methods

113 We see from the previous section that estimating climate change impact just based on the UHI and Urban area  
 114 coverage as in Table 1, cannot take into account solar heating building sidewall areas, massive heat capacities, the  
 115 humidity effects, wind reduction and the solar canyon effect which amplify UHI effects beyond its own climate area.

### 118 2.1 UHI Area Amplification Factor

119 In order to estimate the UHI amplification effects, it is logical to first look at UHI footprint (FP) studies as they  
 120 provide some measurement information. Zhang et al. (2004) found the ecological footprint of urban land cover  
 121 extends beyond the perimeter of urban areas, and the footprint of urban climates on vegetation phenology they found  
 122 was 2.4 times the size of the actual urban land cover. In a more recent study by Zhou et al. (2015), they looked at  
 123 day-night cycles using temperature difference measurements. In this study they found UHI effect decayed  
 124 exponentially toward rural areas for majority of the 32 Chinese cities. Their study was very thorough and extended  
 125 over the period from 2003 to 2012. They describe China as an ideal area to study since it has experienced the  
 126 rapidest urbanization in the world in the decade they evaluated. They found that the “footprint” of UHI effect,  
 127 including urban areas, was 2.3 and 3.9 times of urban size for the day and night, respectively. We note that the  
 128 average day-night amplification footprint coverage factor is 3.1.

130 Looking at Table 2, we see that the UHI Amplification Factor ( $AF_{UHI}$ ) is highly complex making it difficult to assess  
 131 from first principles as it would be some function of Table 2 components:

$$132 AF_{UHI \text{ for } 2019} = f\left(\overline{Build}_{Area} \times \overline{Build}_{C_p} \times \overline{R}_{wind} \times \overline{LossE}_{vtr} \times \overline{Hy} \times \overline{S}_{canyon}\right) \quad (1)$$

133 were

134  $\overline{Build}_{Area}$  = Average building solar area

135  $\overline{Build}_{C_p}$  = Average building heat capacity

136  $\overline{R}_{wind}$  = Average city wind resistance

137  $\overline{LossE}_{vtr}$  = Average loss of evapotranspiration to natural cooling & loss of wetland

138  $\overline{Hy}$  = Average humidity effect due to hydro-hotspot

139  $\overline{S}_{canyon}$  = Average solar canyon effect

140 As a helpful example, one basic formulation that might be suggested is a product of power law average ratios over  
 141 all urban cities compared to a reference year (1950) such that  
 142  
 143

$$144 AF_{UHI \text{ for } 2019} = \left(\frac{(\overline{Build}_{Area})_{2019}}{(\overline{Build}_{Area})_{1950}}\right)^{N_1} \left(\frac{(\overline{Build}_{C_p})_{2019}}{(\overline{Build}_{C_p})_{1950}}\right)^{N_2} \left(\frac{(\overline{R}_{wind})_{2019}}{(\overline{R}_{wind})_{1950}}\right)^{N_3} \left(\frac{(\overline{LossE}_{vtr})_{2019}}{(\overline{LossE}_{vtr})_{1950}}\right)^{N_4} \left(\frac{(\overline{Hy})_{2019}}{(\overline{Hy})_{1950}}\right)^{N_5} \left(\frac{(\overline{S}_{canyon})_{2019}}{(\overline{S}_{canyon})_{1950}}\right)^{N_6} \cdot (2)$$

145 In order to provide some estimate of this factor, we note that Zhou et al. (2015) found the FP physical area (km<sup>2</sup>),  
 146 correlated tightly and positively with actual urban size having correlation coefficients higher than 79%. This  
 147 correlation can be used to provide an initial estimate of this complex factor. Area estimates have been obtained in  
 148 the next Section in Table 3 between 2019 and 1950 time frames. These yield the following results for the Schneider  
 149 et al. (2009) and the GRUMP (2005) extrapolated area results:  
 150

$$151 AF_{UHI \text{ for } 2019} = \frac{(\text{Urban Size})_{2019}}{(\text{Urban Size})_{1950}} \approx \begin{cases} \left(\frac{[0.188]_{2019}}{[0.059]_{1950}}\right)_{Schneider} = 3.19 \\ \left(\frac{[0.952]_{2019}}{[0.316]_{1950}}\right)_{GRUMP} = 3.0 \end{cases} \quad (3)$$

152 Between the two studies, the UHI area amplification factor average is 3.1. Coincidentally, this is the same factor  
 153 observed in the Zhou et al. (2015) study for the average footprint. This factor may seem high. However, it is likely  
 154 conservative. There are other effects that would be difficult to assess. For example, increases in global draught due  
 155 to loss of wet lands, deforestation effects due to urbanization and draught related fires. It could also be important to  
 156 factor in changes of other impermeable surfaces since 1950 such as highways, large impermeable surfaces (parking  
 157 lots and event centers), and so forth.

158  
 159 **2.2 Alternate Method Using the UHI’s Horizontal Extent**  
 160

161 An alternate approach to check the estimate of Equation 3, is to look at the UHI’s horizontal extent. Fan et al. (2017)  
 162 using an energy balance model to obtain the maximum horizontal extent of a UHI heat dome in numerous urban  
 163 areas found the nighttime extent of 1.5 to 3.5 times the diameter of the city’s urban area (2.5 average) and the  
 164 daytime value of 2.0 to 3.3 (2.65 average).

165  
 166 Applying this energy method (instead of the area ratio factor in Eq. 3), yields a diameter in 2019 compared to that of  
 167 1950 increase of about 1.8. This implies a factor of  $2.5 \times 1.8 = 4.5$  higher in the night and  $2.65 \times 1.8 = 4.8$  in the day in  
 168 1950 (average 4.65). This increase occurs 62.5% of the time according to Fan et al., (where their steady state  
 169 occurred about 4 hours after sunrise and about 5 hours after sunset) yielding an effective UHI amplification factor of  
 170 2.9. We note this amplification factor is in good agreement with Equation 3. The fact that it is a bit lower may be  
 171 because Fan et al. only assessed the steady state region, one would anticipate some increase from the non-steady  
 172 state period.

173  
 174 **2.3 Area Extrapolations for 1950 and 2019**  
 175

176 In order to assess the urbanized area, (also used in determining the UHI amplification factor ratios above), we need  
 177 to project the Schneider and GRUMP area estimates down to 1950 and up to 2019. Both use datasets from around  
 178 2000 so this is a convenient somewhat middle time-frame. Here we decided to use the world population growth rate  
 179 (World Bank 2018) which varies by year as shown in Appendix A in Figure A1. We used the average growth rate  
 180 per ½ decade for iterative projections (about 1.3% to 1.6% per year).

181  
 182 To justify this we see that Figure A2a illustrates that building material aggregates (USGS 1900-2006) used to build  
 183 cities and roads correlates well to population growth (US Population Growth 1900-2006).

184  
 185 **Table 3.** Extrapolated and amplified urbanized coverage estimates

Year	Urban coverage percent of Earth	Amplification factor effect	Effective amplification coverage area effect
Schneider study			
1950	0.059*	1	0.059%
2000-2001	$0.0051 \times 29\% = 0.148$		
2019	0.188*	3.1 AF <sub>UHI</sub> **	<b>0.583%</b>
Worst case GRUMP study			
1950	0.316%*	1	<b>0.316%</b>
2000	$0.027 \times 29\% = 0.783\%$		
2019	0.952%*	3.1 AF <sub>UHI</sub> **	<b>2.95%</b>

186 \*Growth rate of cities using world population yearly growth rate in Fig A1, \*\*AF<sub>UHI</sub> is the area  
 187 amplification factor for 2019 referenced to 1950.  
 188

189 It is also interesting to note that building materials for cities and roads also correlates well to global warming trends  
 190 (NASA 1900-2006) shown in Figure A2b.

191  
 192 Column 2 in Table 3 show the projections with the actual year (~2000) data point tabulated value also listed in the  
 193 table (also see Table 1). The UHI area amplification factor of 3.1 (Column 3) are then applied to Schneider and  
 194 GRUMP studies shown in Column 4.

197 **2.4 Weighted Amplification Albedo Solar Urbanization (WAASU) Model Overview**

198  
 199 The WAASU model is very straightforward; it is based on a global weighted albedo model. The Earth Albedo is  
 200 given by

201 
$$Earth\ Albedo = \sum_i \{ \%Effective\ Surface\ Area_i \times Surface\ Item\ Albedo_i \} + Cloud\ Area \times Cloud\ Albedo. \quad (4)$$

202 Here the effective surface area is given by

203  
 204 
$$Effective\ Surface\ Area = Surface\ Area \times \%Solar\ Irradiance. \quad (5)$$

205  
 206 We note that the change in the Earth Albedo change over time (from 1950 to 2019), is just a function of the UHI  
 207 area variation, (when holding all unrelated UHI components fixed), that is

208  
 209 
$$\left( \frac{dEA}{dt} \right)_{EA'} = \sum_i \left( Albedo_{UHI} \times Solar\ Irradiance \times \frac{dArea_{UHI}}{dt} \right)_i, \quad (6)$$

210  
 211 where EA is the Earth Albedo, and EA' are all other Earth components (held fixed). Although it is possible that the  
 212 solar irradiance percent changes due to new city locations, in this model we assume it is fixed at 100%. This  
 213 indicates, for example, that even if we were to change the *Effective Surface Area* of perhaps the *sea ice component*  
 214 due to the fact that it receives about 40% irradiance compared with other areas and redistributed its radiance (per the  
 215 Earth's energy budget), it would not affect the overall results when looking at the albedo change due to the UHI  
 216 effect from 1950 to 2019. Therefore, the model allows freedom to only work with normalized area coverage changes  
 217 when focusing on the UHI effect. On the other hand, solar irradiance comes into play for sea ice when we are  
 218 considering its global albedo effect from 1950 to 2019 (see Appendix C). However, the solar radiation weighting,  
 219 albedo, and areas for all Earth components are subjected to the constraints below.

220  
 221 **2.4.1 Model Constraints**

222  
 223 This model is subject to the constraint

224 
$$Total\ Area = \sum_i \{ \%Earth\ Surface\ Areas_i \} + \%Cloud\ Area = 100\% \quad (7)$$

225  
 226 and the normalization constraint for the Earth surface areas (when the UHI area is increased) must then be subject to

227  
 228 
$$\sum_i \{ \%Earth\ Surface\ Areas_i \} = 100\% - \%Cloud\ Area. \quad (8)$$

229  
 230 To simplify things as much as possible, only five Earth constituents are used: *water*, *sea ice*, *land*, *UHI coverage*,  
 231 *and clouds* (where *land* is its area minus the UHI coverage). These components are fairly easy to estimate and  
 232 references for their values are provided in Appendix D. Furthermore, we use consistent values found in the IPCC  
 233 AR5 report (Hartmann et al., 2013) assessment of the Earth's energy budget for solar irradiance. Table 4  
 234 summarizes the constraints from these IPCC values.

235  
 236 The fixed components of our model maintain relative consistency from 1950 to 2019. The non-fixed value is the  
 237 urban coverage as indicated by Equation 6. The only unknown value is the *land* albedo (minus the UHI coverage)  
 238 and this value is adjusted to obtain the IPCC global albedo of 29.4118% and its *land* value of incident/reflected  
 239 value of 7.0588.

240 **Table 4. IPCC Earth energy budget values (Hartmann et al., 2013)**

IPCC Item	Incident and Reflected Radiation (W/m <sup>2</sup> )	Albedo %	Absorbed (W/m <sup>2</sup> )
Earth	100/340	<b>29.4118</b>	240=340x(1-.294)
Atmosphere & Clouds	76/340	<b>22.3529</b>	<b>79</b>
Earth Surface Albedo	24/340	<b>7.0588</b>	<b>161</b>

241  
 242

243 These values are used as a 1950 starting point and then the 2019 increase for UHI coverage area is inserted. This  
 244 increases the Earth's area to greater than 100%. Therefore, renormalization is done per the constraint of Equation 8  
 245 (detailed in Appendix B).

246  
 247 **3 Results and discussion**  
 248

249 Using the extrapolated area coverage in Table 3 with the 3.1 amplification factor applied to the urbanized growth,  
 250 the resulting global albedo change occurred of 29.3956% in 2019 (Table 5b) compared to the earlier 1950 albedo  
 251 value of 29.4118% (Table 5a) for the Schneider nominal case. As well, for the GRUMP worst case, the albedo  
 252 changed from 29.4118% (Table 6a) to 29.3322% (Table 6b) due to the urbanized growth.

253  
 254 As we mentioned earlier, the increases in the solar surface area of the Earth, which will occur with city growth of  
 255 tall buildings and their solar areas, however comparatively small, requires renormalization in the model of the Earth  
 256 surface components of the WAASU model (detailed in Appendix B). This is displayed in column 3 in Tables 5b and  
 257 6b. While the model is sensitive to urban coverage changes, it works well with renormalization showing a high level  
 258 of consistency to urban coverage proportionality changes. This is indicated in Table 7 where we find the GRUMP  
 259 2019 area sensitivity is 0.0944%Norm Area/(W/m<sup>2</sup>) (=0.271/2.87) compared with the Schneider area sensitivity of  
 260 0.0948 %Norm Area/(W/m<sup>2</sup>) (=0.055/0.58).

261  
 262 **Table 5a.** Schneider results (Albedo=29.4118, 1950)      **Table 5b.** Schneider results (Albedo=29.3956%, 2019)

Surface	Albedo	% Area of Surface	Normalized Earth Area	Weighted Albedo %
	<b>A</b>	<b>B</b>	<b>C=A x B x (1-0.67)</b>	<b>A x C</b>
Sum of Water Type		71		
Sea Ice	0.6	15	4.95	2.970
Water	0.06	56	18.48	1.109
Sum of Land Type		29		
Land - (UHI + Coverage)	0.3118	28.941	9.55053	2.978
UHI + Coverage	0.12	0.059	0.01947	0.002
		Σ=100.000	33.000	7.05882
			Cloud Area	
Clouds	0.3336	67	67	22.35294
Σ Sum Earth %			100.000	
Σ Global Albedo				29.4118

Surface	Albedo	Normalized % Surface Area	Normalized Earth Area	Weighted Albedo %
	<b>A</b>	<b>B</b>	<b>C=A x B x (1- 0.67)</b>	<b>A x C</b>
Sum of Water Type		70.6298		
Sea Ice	0.6	14.9218	4.924194	2.955
Water	0.06	55.7081	18.383673	1.103
Sum of Land Type		29.37		
Land - (UHI + Coverage)	0.3118	28.79	9.5007	2.962
UHI + Coverage	0.12	0.58	0.1914	0.023
		Σ=100.000	33.000	7.0197
			Cloud Area	
Clouds	0.3336	67	67	22.3529
Σ Sum Earth %			100.000	
Σ Global Albedo				29.3956

263

264 **Table 6a.** GRUMP results (Albedo=29.4118, 1950)      **Table 6b.** GRUMP results (Albedo=29.3322%, 2019)

Surface	Albedo	% Surface Area	Normalized Earth Area	Weighted Albedo %
	<b>A</b>	<b>B</b>	<b>C=A x B x (1-0.67)</b>	<b>A x C</b>
Sum of Water Type		71		
Sea Ice	0.6	15	4.95	2.970
Water	0.06	56	18.48	1.109
Sum of Land Type		29		
Land - (UHI + Coverage)	0.3135	28.684	9.46572	2.968
UHI + Coverage	0.12	0.316	0.10428	0.013
Sum Surface %		Σ=100.000	33.000	7.0588
			Cloud Area	
Clouds	0.3336	67	67	22.3529
Σ Sum Earth %			100.000	
Σ Global Albedo				29.4118

Surface	Albedo	Normalized % Surface Area	Normalized Earth Area	Weighted Albedo %
	<b>A</b>	<b>B</b>	<b>C=A x B x (1- 0.67)</b>	<b>A x C</b>
Sum of Water Type		69.1778		
Sea Ice	0.6	14.615	4.82295	2.894
Water	0.06	54.5628	18.005724	1.080
Sum of Land Type		30.8221		
Land - (UHI + Coverage)	0.3135	27.9478	9.222774	2.891
UHI + Coverage	0.12	2.8743	0.948519	0.114
Sum Earth %		Σ=100.000	33.000	6.8655
			Cloud Area	
Clouds	0.3336	67	67	22.3529
Σ Sum Earth %			100.000	
Σ Global Albedo				29.3322

265

266 Table 7 provides a summary of albedo changes found in the WASSU model along with the expected solar long wave  
 267 radiation increase. From the above global WAASU model, the estimates of the Earth's radiated long wavelength  
 268 emissions are set equal to the short wave radiation absorption:

269  
 270 
$$P_{Total} = 340 \text{ W/m}^2 (1 - \text{Albedo}). \tag{9}$$

271  
 272 Then the change from 1950 to 2019 represents the equivalent increase in long wave radiation is given by

273  
274  
275  
276  
277  
278  
279  
280

$$\Delta P_{Total} = 340 \text{ W/m}^2 \{ (1-\text{Albedo})_{2019} - (1-\text{Albedo})_{1950} \}. \tag{10}$$

Results are compiled in Table 7. The table also includes “what if” estimates, if we could change urbanization to be more reflective with cool roofs to reverse the effect.

**Table 7.** Albedo and radiative increase model results with UHI effective area.

Year	Urban Extent Global Area %	UHI Effective Global Surface % Area	Normalized UHI Effective Global Surface % Area	Albedo Cities	Global Weighted Albedo	$\Delta P_{Total}$ UHI Radiative Increase $\text{W/m}^2$ (%GW)*	Sensitivity $\frac{W}{m^2 \cdot K}$	Model Area Sensitivity $\frac{\Delta P_{Total} (W/m^2)}{Norm\% Area}$
Nominal Case IPCC Schneider 2009 Study								
1950	0.059	0.059	0.059	0.12	29.4118	0	—	—
2019	.188	0.583	0.58	0.12	29.3978	0.055 (1.54%)*	0.058	0.0948
What if	0.188	0.583	0.58	0.204	29.4118	-0.055 (-1.54%)*	-0.058	—
Worst Case GRUMP 2005 Study								
1950	0.316%	0.316	0.316	0.12	29.4118	0	—	—
2019	0.952%	2.95	2.8743	0.12	29.3322	0.271 (7.6%)*	0.285	0.0944
What if	0.952%	2.95	2.8743	0.2039	29.4118	-0.271 (-7.6%)*	-0.285	—

\*Percent of Warming estimate,  $P=340 \times (1-\text{Albedo})$ ,  $\%GW = \{ (P/\epsilon\sigma)_{2019}^{0.25} - (P/\epsilon\sigma)_{1950}^{0.25} \} / 0.95^\circ\text{C}$ ,  $\epsilon=1$

281  
282  
283  
284  
285  
286  
287  
288  
289  
290  
291

The general results are summarized:

- Nominal Schneider case from 1950 to 2019 is  $0.055 \text{ W/m}^2$  due to urban amplification coverage. This would equate to about 1.55% of global warming assuming the total increase from 1950 is about  $0.95^\circ\text{C}$  in 2019.
- Worst GRUMP case from 1950 to 2019 is  $0.271 \text{ W/m}^2$  due to urban amplification coverage. This would roughly equate to about 7.5% of global warming assuming the total increase from 1950 is about  $0.95^\circ\text{C}$  in 2019.
- “What if” corrective action results of cool roofs indicates that changing city albedos in both the Schneider and the GRUMP case from 0.12 to 0.204 would reverse the increase in emission back to 1950 levels.

Model consistency is indicated in the area sensitivity column in Table 7. Furthermore, we note that radiation increase goes as the area changes. That is, the Schneider to Grump normalized area increase from 0.58 (Schneider) to 2.8743% (GRUMP) yields a factor of 3.96  $(= (2.874 - .58) / .58)$ . This can be compared to the observed long radiation increase from  $0.055 \text{ W/M}^2$  (Schneider) to  $0.271 \text{ W/M}^2$  (GRUMP) that also yields a similar factor of 3.93  $(= (0.271 - .055) / .055)$ . This observation along with the area sensitivity values can be helpful in estimating future warming trends due to UHI growth rates, which at the present time from Figure A1, is about 1.2% per year. We also note that in both the Schneider and GRUMP case, implementing cool roof requires the same albedo change from 0.12 to 0.204 in order to reverse the warming trend.

300  
301  
302  
303  
304

Although global warming assessment obtained in the WAASU model, especially for the Schneider case does not appear to show much contribution to global warming, we find that climate sensitivity feedback estimates increase the UHI effective contribution significantly. Suggestions in Appendix C indicate that the root cause global warming contribution may go as high as 5% for the Schneider case and 24% for the GRUMP case (see Table C2).

#### 305 306 4 Conclusions

307  
308  
309  
310  
311  
312

In this paper we were able to estimate using UHI effect (with urban area) amplification coverage estimates with the aid of estimated UHI amplification factors. These estimates inserted into our WAASU model found that between  $0.055$  and  $0.271 \text{ W/m}^2$  of radiative forcing is possible according the WAASU model (this results indicates that about 1.6 and 7.5% of global warming may be due to the UHI effect (with urban areas). The model found that the effect was proportional to the UHI amplification area coverage with area sensitive estimate was about 0.095

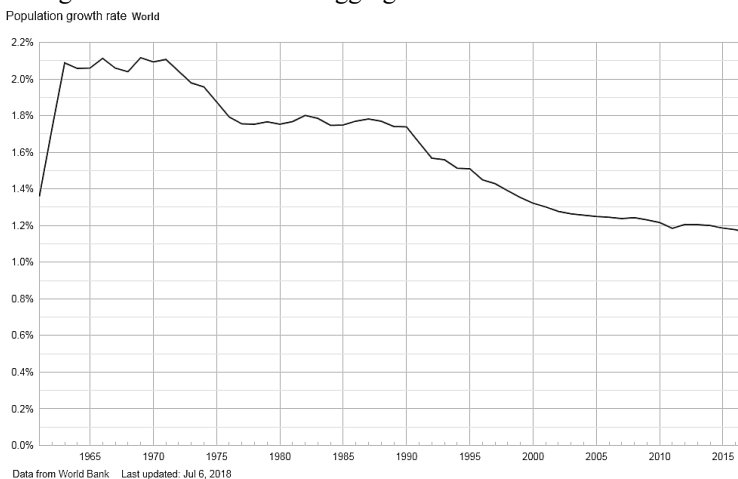
313 (W/m<sup>2</sup>)/%Normalized Area. Examples are provided in Appendix C to illustrate how the UHI root-cause global  
 314 warming can increase significantly when climate feedback factor contributions are considered. As area estimates  
 315 and UHI amplification factors are very sensitive to the final results, it is clear refined values of both would be  
 316 important for further study.

317  
 318 Below we provide suggestions and corrective actions which include:

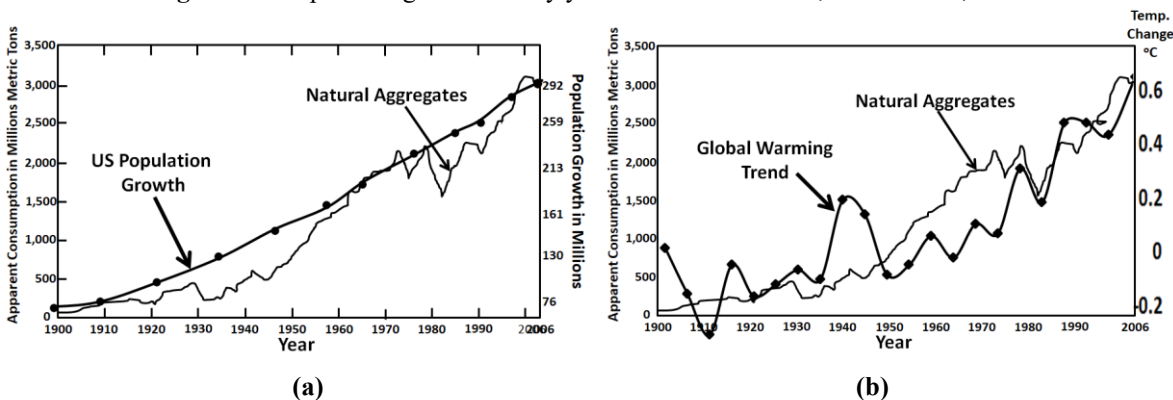
- 319 • IPCC be more proactive in helping to providing albedo guidelines or recommendation similar to their CO<sub>2</sub>  
 320 effort for both UHIs and roads.
- 321 • A guideline for future albedo design requirements of city and roads should be developed.
- 322 • Recommend an agency like NASA be tasked with finding applicable solutions to cool down UHIs.
- 323 • Recommendation for cars to be more reflective. Here although world-wide cars likely do not embody much  
 324 of the Earth's area, recommending that all new manufactured cars be higher in reflectivity (e.g., silver or  
 325 white) would help raise awareness of this issue similar to electric cars that help improve CO<sub>2</sub> emissions.

326  
 327 **Appendix A: Growth Rates and Information on Natural Aggregates**  
 328

329 Below is a plot of the world population growth rate that varies from about 2.1 to 1.1. This is used to make growth  
 330 rate estimates of urban coverage. We note that natural aggregate used to build cities and roads are reasonably  
 331 correlated to population growth in Figure A2a. Also of interest (Fig. A2b) is the fact that one can see some  
 332 correlation to global warming with the use of natural aggregates.



333  
 334 **Figure A1.** Population growth rate by year from 1960 to 2018, World Bank, 2018



335  
 336 **Figure A2. a)** Natural aggregates correlated to U.S. Population Growth (USGS 1900-2006) **b)** Natural aggregates  
 337 correlated to global warming (NASA 2020)  
 338

339  
 340  
 341  
 342  
 343 **Appendix B: Albedo Model Renormalization Information**  
 344

345 Table 5a and b are reproduced to illustrate the renormalization method.  
 346



347 **Table 5a.** Schneider results (Albedo=29.4118, 1950) **Table 5b.** Schneider results (Albedo=29.3956%, 2019)

Surface	Albedo	% Area of Surface	Normalized Earth Area	Weighted Albedo %
	A	B	$C=A \times B \times (1-0.67)$	A x C
Sum of Water Type		71		
Sea Ice	0.6	15	4.95	2.970
Water	0.06	56	18.48	1.109
Sum of Land Type		29		
Land - (UHI + Coverage)	0.3118	28.941	9.55053	2.978
UHI + Coverage	0.12	0.059	0.01947	0.002
		$\Sigma=100.000$	33.000	7.05882
			Cloud Area	
Clouds	0.3336	67	67	22.35294
$\Sigma$ Sum Earth %			100.000	
$\Sigma$ Global Albedo				29.4118

Surface	Albedo	Normalized % Surface Area	Normalized Earth Area	Weighted Albedo %
	A	B	$C=A \times B \times (1-0.67)$	A x C
Sum of Water Type		70.6298		
Sea Ice	0.6	14.9218	4.924194	2.955
Water	0.06	55.7081	18.383673	1.103
Sum of Land Type		29.37		
Land - (UHI + Coverage)	0.3118	28.79	9.5007	2.962
UHI + Coverage	0.12	0.58	0.1914	0.023
		$\Sigma=100.000$	33.000	7.0197
			Cloud Area	
Clouds	0.3336	67	67	22.3529
$\Sigma$ Sum Earth %			100.000	
$\Sigma$ Global Albedo				29.3956

348 Renormalization is done as follows:

- 349 1. Model starts with 1950 Table 5a albedo 29.4118%, then 2019 urban coverage area is entered.
- 351 2. For example, in Table B1, the new area increases from 0.59% to .583%. This is 0.525% larger, now
- 352 the ‘Sum of % of Earth Area’ will be 100.527% in 2019.
- 353 3. All areas are renormalized to 101.527%. For example, sea ice at 15% in 1950 becomes
- 354  $15\% \times (100.000/100.527) = 14.921\%$  and the Urban Coverage becomes  $0.583\% \times (100/101.11) = 0.58\%$ .

355 **Appendix C: Related Warming Estimates and Other Amplification Factors**

356 Although the results obtained here at first seem to indicate that UHIs do not appear to contribute much to global

357 warming, when other amplification factors are considered, much stronger significance will be estimated. In this

358 appendix, additional feedback factors are suggested providing a number of global warming estimates.

- 359 • *Such factors can be contentious; therefore we have chosen to provide these in this appendix mainly as*
- 360 *an aid for the reader to illustrate how climate sensitivity can factor into the magnitude of UHIs warming*
- 361 *significance. These estimates should be considered only as ballpark values.*

362 **C.1 Global Feedback Amplification Factors**

363 There is a wide range of possible estimates of climate feedback sensitivity driven by uncertainties in how water

364 vapor, clouds, and other factors change as the Earth warms. Climate feedbacks are mixed and some will amplify

365 (positive feedback) or diminish the effect of warming from the root cause effects (see for example Hausfather 2018).

366 The actual feedback is known to be positive (van Nes, 2015). Climatologists will often approximate such factors

367 frequently in reference with CO<sub>2</sub> doubling theory as positive. For example, water-vapor feedback alone, which is

368 one of the most important in our climate system, is thought to have the capacity to about double the direct warming

369 (Manabe and Wetherald, 1967; Randall et al., 2007, Dessler et. Al, 2008). This results from the fact that warm air

370 holds more greenhouse moisture gas. Climate models incorporate this feedback. Water vapor feedback is strongly

371 positive, with most evidence supporting a magnitude of 1.6 to 2.0 W/m<sup>2</sup>/K (Dessler et. al., 2008). Also water vapor

372 feedback is considered a faster feedback mechanism (Hansen, 2008). We will use a factor of 1.75, a bit less than a

373 doubling factor of 2. This factor would apply equally to UHI warming contribution, Greenhouse Gases (GHG), or

374 warming due to sea ice melting.

375 **C.2 WAASU Model Applied to the Melting of Sea Ice**

376 While the Antarctic sea ice has remained roughly constant, the Arctic sea ice is melting at an alarming rate of

377 12.85% in the last two decades (NASA sea ice, 2019). This apparent trend appears to yield about a 26% change in

378 sea ice loss. It is difficult to find a strong reference for quantifying global warming impact due to Arctic sea ice

379 melting. However, we might get a rough ballpark approximation by this WAASU model (and also illustrate one of

380 the strengths of the model). Sea ice melting will results in a significant albedo change roughly from ice albedo of

381 0.6, to the open ocean albedo of 0.06 (see Table C1 and C2). Fortunately, the Arctic areas receive only about 40% as

389 much solar radiation (Sciencing, 2018) reducing the feedback effect. From Equation 5, the effective sea ice surface  
 390 area reduction from the irradiance decrease can be approximated as

391  
 392 Effective sea ice surface area= 15% (1-0.26 x 0.40)=13.44% (a 1.56% reduction of effective area). (C-1)  
 393

394 In the WAASU model, we will have to make an assumption that the effective ocean surface area increases  
 395 proportionately by 1.56% to 57.56% (see Table C2). The model then finds that the global albedo change decreases  
 396 from 29.4118 to 28.9948%. (Note that alternately we could have set the albedo to 29.4118% in 2019 and worked  
 397 back to 1950. In this case the albedo would have increase to 29.83%).  
 398

399 **Table C1.** Schneider results (Albedo=29.4118, 1950) **Table C2.** Sea ice loss - albedo change (29.0643%, 2019)

Surface	Albedo	% Area	Normalized	Weighted
		of Surface	Earth Area	Albedo %
	A	B	C=A x B x (1-0.67)	A x C
Sum of Water Type		71		
Sea Ice	0.6	15	4.95	2.970
Water	0.06	56	18.48	1.109
155Sum of Land Type		29		
Land - (UHI + Coverage)	0.3118	28.941	9.55053	2.978
UHI + Coverage	0.12	0.059	0.01947	0.002
		Σ=100.000	33.000	7.05882
			Cloud Area	
Clouds	0.3336	67	67	22.35294
Σ Sum Earth %			100.000	
Σ Global Albedo				29.4118

Surface	Albedo	Normalized	Normalized	Weighted
		% Surface Area	Earth Area	Albedo %
	A	B	C=A x B x (1-0.67)	A x C
Sum of Water Type		71		
Sea Ice	0.6	13.44	4.4352	2.507
Water	0.06	57.56	18.9948	1.14
Sum of Land Type		29	23.43	
Land - (UHI + Coverage)	0.3118	28.941	9.55053	2.978
UHI + Coverage	0.12	0.059	0.01947	0.002
		100.000	33.000	6.6395
			Cloud Area	
Clouds	0.3336	67	67	22.3530
Σ Sum Earth %			123.430	
Σ Global Albedo				29.1338

400  
 401 The Global Warming (GW) is found as:  
 402

403 
$$\%GW = \{(P/\epsilon\sigma)^{0.25}_{2019} - (P/\epsilon\sigma)^{0.25}_{1950}\} / 0.95^{\circ}C, \quad (C-2)$$

404  
 405 where  $P=340W/m^2 \times (1-Albedo)$  and  $\epsilon=1$ . The warming increase due to ice melting is estimated from this model to  
 406 be about 0.25°C or 26.4% of the 0.95 °C increase in 2019.

407  
 408 This estimate should only be taken as ballpark due to numerous uncertainties as climatologists find it hard to fully  
 409 quantify the seasonal variations in ice change and to know the possible impact on cloud coverage increase from  
 410 additional warming evaporation. However, one would expect less evaporation in the Arctic. Thus, there are a lot of  
 411 uncertainties.

412  
 413 **C.3 Ballpark Contributions to Global Warming**  
 414

415 Table C3 summarizes the key global warming cause and effect factors that we have described.

416  
 417 **Table C3.** Global warming factors of interest

Urban Climate Amplification	Effects	Where Applied
UHI Area Amplification Factor	3.1 UHI Amplification	Applied to 2019 UHI Area
UHI Dome Horizontal Method	2.9 UHI Amplification	Applied to 2019 UHI Area
Ice Melting	0.25°C	25 °C out of 0.95 °C
Atmospheric Moisture Increase	1.75 GW Amplification	Applied to Ice Melting Temp, UHI, and GHGs +X*

418 where X is any other feedbacks (positive or negative)

419  
 420 Then major contributions to global warming can be simplified as follows  
 421

422 
$$\Delta T_{GW} = \frac{\Delta F}{\lambda} = \Delta T_{UHI} + \Delta T_{Water-Vapor} + \Delta T_{Sea-Ice} + \Delta T_{GHG+X}, \quad (C-3)$$

424 where  $\Delta T_{GW}=0.95^{\circ}C$ ,  $\Delta T_{UHI-Schneider}=0.0147^{\circ}C$  (Table 7),  $\Delta T_{Sea-Ice}=0.25^{\circ}C$ ,  $\lambda$  is the climate sensitivity, and  $\Delta F$  is the  
 425 radiative forcing change. We have two unknowns  $\Delta T_{Water-Vapor}$  and  $\Delta T_{GHG+X}$ . Here X are other feedback mechanisms  
 426 like increases in cloud coverage so it can be both positive or negative. These two unknowns may be estimated from  
 427 the following two equations

428  
 429 
$$0.95^{\circ}C = AF_{water\ vapor} \times (\Delta T_{UHI} + \Delta T_{GHG+X} + \Delta T_{Sea-Ice}) = 1.75 (0.0147^{\circ}C + \Delta T_{GHG+X} + 0.25^{\circ}C) \quad (C-4)$$

430 and

431 
$$0.95^{\circ}C = \Delta T_{UHI} + \Delta T_{GHG+X} + \Delta T_{Sea-Ice} + \Delta T_{Water-Vapor} = 0.0147^{\circ}C + \Delta T_{GHG+X} + 0.25^{\circ}C + \Delta T_{Water-Vapor}. \quad (C-5)$$

432  
 433 The water vapor  $AF_{water-vapor}=1.75$  is discussed above. Then solving, the results are tabulated in the Table C3. We  
 434 note that in terms of root-causes, these suggested values indicate that the UHI effect (with coverage) with global  
 435 warming contributions are responsible for between 5 to 24% of global warming.

436  
 437 **Table C3. Global warming contributions (2019)**

Warming Component	Temperature Contribution (°C)	Percent of GW Root Cause	Percent of GW	Radiative Forcing W/m <sup>2</sup>
<b>Schneider Study</b>				
Urbanization	0.0146	<u>5</u>	1.54	0.055
Greenhouse gases + X	0.278	95	29.3	1.5
Sea ice melting feedback	0.25		26.3	1.35
Water vapor feedback	0.4073		42.9	2.19
<b>Total</b>	<b>Σ0.95</b>			5.1
<b>GRUMP Study</b>				
Urbanization	0.0713	<u>24.4</u>	7.6%	0.271
Greenhouse gases + X	0.2215	75.6	23	1.19
Sea ice melting feedback	0.25		26	1.25
Water vapor feedback	0.407		43	2.19
<b>Total</b>	<b>Σ0.95</b>			4.9

438  
 439 From the table the UHI effective feedback sensitivity contribution is about 3.2 (5%/1.54% or 24%/7.6%). This also  
 440 indicated that the UHI area sensitivity would increase by 3.2 from 0.094 to about 0.3 W/m<sup>2</sup>/%Normalized Area (see  
 441 Table 7).

442  
 443 Often, we would like an estimate of the GHG effect related to CO<sub>2</sub>. If we assume the CO<sub>2</sub> is responsible for about  
 444 1/3 of global warming, we find for the Schneider case (with GHG ≈ CO<sub>2</sub>)

445  
 446 
$$\Delta T_{CO2+X} = 0.278^{\circ}C = \Delta T_{CO2} + \Delta T_X = 0.32^{\circ}C + (-.042^{\circ}C) \quad (C-6)$$

447 and for the GUMP case

448 
$$\Delta T_{CO2+X} = 0.2215^{\circ}C = \Delta T_{CO2} + \Delta T_X = 0.32^{\circ}C + (-.0985^{\circ}C) \quad (C-7)$$

449  
 450 Although these values are crude estimates, they serve as possible examples.

451  
 452 **Appendix D: WAASU Model References**

453  
 454 Table D1 provides references for the WAASU model values.

455  
 456 **Table D1 Key References for WAASU model**

Parameter	Albedo (reference)	1950 Area (reference)
Sea Ice	50-70%, average 60% (NSID 2020)	15% (Lindsey 2019)
Water	0.06 (NSIDC 2020)	56% Ocean+Sea Ice=71% (USGS)
Land-(UHI+Coverage)	Adjusted to obtain 29.412% and surface reflected of 7.06 Earth Albedo in 1950 thereafter held fixed (see IPCC Hartmann (2013) AR5 report)	29%-Urban Coverage
UHI+Cov	0.12 Sugawara et. Al (2014)	See Table 1
Clouds	22.35294 (IPCC Hartmann et al., 2013)	67% (Earthobservatory, NASA)

457  
458459 **References**

460

461 Barr J. M., 2019 The Economics of Skyscraper Height (Part IV): Construction Costs Around the World,  
462 <https://buildingtheskyline.org/skyscraper-height-iv/>463 Basara J. ,P. Hall Jr. , A.Schroeder , B.Illston ,K.Nemunaitis 2008, Diurnal cycle of the Oklahoma City urban heat  
464 island, J. of Geophysical Research465 Cao C.X. , Zhao J., P. Gong, G. R. MA, D.M. Bao, K.Tian, Wetland changes and droughts in southwestern China,  
466 Geomatics, Natural Hazards and Risk, Oct 2011,467 <https://www.tandfonline.com/doi/full/10.1080/19475705.2011.588253>468 Cormack L. 2015 Where does all the stormwater go after the Sydney weather clears? The Sydney Morning Herald,  
469 [https://www.smh.com.au/environment/where-does-all-the-stormwater-go-after-the-sydney-weather-clears-](https://www.smh.com.au/environment/where-does-all-the-stormwater-go-after-the-sydney-weather-clears-20150430-1mx4ep.html)

470 20150430-1mx4ep.html

471 Dessler A. E. ,Zhang Z., Yang P., Water-vapor climate feedback inferred from climate fluctuations, 2003–2008,  
472 *Geophysical Research Letters*, (2008), <https://doi.org/10.1029/2008GL035333>473 Earthobservatory, NASA (clouds albedo 0.67) <https://earthobservatory.nasa.gov/images/85843/cloudy-earth>474 Fan, Y., Li, Y., Bejan, A. *et al.* Horizontal extent of the urban heat dome flow. *Sci Rep* 7, 11681 (2017).  
475 <https://doi.org/10.1038/s41598-017-09917-4>476 Feddema, J. J., K. W. Oleson, G. B. Bonan, L. O. Mearns, L. E. Buja, G. A. Meehl, and W. M. Washington (2005),  
477 The importance of land-cover change in simulating future climates, *Science*, **310**, 1674– 1678,  
478 doi:10.1126/science.1118160479 Galka M. 2016, Half the World Lives on 1% of Its Land, Mapped, [https://www.citylab.com/equity/2016/01/half-](https://www.citylab.com/equity/2016/01/half-earth-world-population-land-map/422748/)480 earth-world-population-land-map/422748/, (2016 publication on 2000 data set, [http://metrocosm.com/world-](http://metrocosm.com/world-population-split-in-half-map/)

481 population-split-in-half-map/

482 Global Rural Urban Mapping Project (GRUMP) 2005, Columbia University Socioeconomic Data and Applications

483 Center, Gridded Population of the World and the Global Rural-Urban Mapping Project (GRUMP).

484 Hansen, J., "2008: Tipping point: Perspective of a climatologist." Archived 2011-10-22 at the Wayback Machine,

485 Wildlife Conservation Society/Island Press, 2008. Retrieved 2010.

486 Hartmann, D.L., A.M.G. Klein Tank, M. Rusticucci, L.V. Alexander, S. Brönnimann, Y. Charabi, F.J. Dentener,

487 E.J. Dlugokencky, D.R. Easterling, A. Kaplan, B.J. Soden, P.W. Thorne, M. Wild and P.M. Zhai, 2013:

488 Observations: Atmosphere and Surface. In: Climate Change 2013: The Physical Science Basis. Contribution of

489 Working Group I to the Fifth Assessment Report of the Intergovernmental Panel on Climate Change [Stocker,

490 T.F., D. Qin, G.-K. Plattner, M. Tignor, S.K. Allen, J. Boschung, A. Nauels, Y. Xia, V. Bex and P.M. Midgley

491 (eds.)]. Cambridge University Press, Cambridge, United Kingdom and New York, NY, USA.

492 Hirshi M. ,Seneviratne S. , V. Alexandrov, F. Boberg, C. Boroneant, O. Christensen, H. Formayer, B. Orlowsky &amp;

493 P. Stepanek, Observational evidence for soil-moisture impact on hot extremes in Europe, *Nature Geoscience* 4,

494 17-21 (2011)

495 Huang Q. , Lu Y. 2015 Effect of Urban Heat Island on Climate Warming in the Yangtze River Delta Urban

496 Agglomeration in China, *Intern. J. of Environmental Research and Public Health* 12 (8): 8773 (30%)

497 Jones, P. D., D. H. Lister, and Q.-X. Li, 2008: Urbanization effects in large-scale temperature records, with an

498 emphasis on China. *J. Geophys. Res.*, 113, D16122, doi: 10.1029/2008JD009916.

499 Lindsey R, Scott M., (2019), Climate Change: Arctic Sea Ice Summer Minimum, NOAA Climate.gov,

500 <https://www.climate.gov/news-features/understanding-climate/climate-change-minimum-arctic-sea-ice-extent>

501 Manabe, S., and R. T. Wetherald (1967), Thermal equilibrium of atmosphere with a given distribution of relative

502 humidity, *J. Atmos. Sci.*, 24, 241–259.

503 McKittrick R. and Michaels J. 2004. A Test of Corrections for Extraneous Signals in Gridded Surface Temperature

504 Data, *Climate Research*

505 McKittrick R., Michaels P. 2007 Quantifying the influence of anthropogenic surface processes and inhomogeneities

506 on gridded global climate data, *J. of Geophysical Research-Atmospheres*507 McKittrick Website Describing controversy: <https://www.rossmckittrick.com/temperature-data-quality.html>508 NASA 1900-2006 updated, 2020 <https://climate.nasa.gov/vital-signs/global-temperature/>509 NASA 2000, Gridded population of the world, , [https://sedac.ciesin.columbia.edu/data/set/gpw-v3-population-](https://sedac.ciesin.columbia.edu/data/set/gpw-v3-population-count/data-download)

510 count/data-download

511 NASA Sea Ice, (2019) <https://climate.nasa.gov/vital-signs/arctic-sea-ice/>512 NSID 2020, National Snow & Ice Data Center, "Thermodynamics: Albedo". [nsidc.org](https://nsidc.org/cryosphere/seaice/processes/albedo.html). Retrieved 14 August 2016.513 <https://nsidc.org/cryosphere/seaice/processes/albedo.html>514 Randall, D. A. *et al.* (2007), Climate models and their evaluation, in *Climate Change 2007: The Physical Science*

515 Basis. Contributions of Working Group I to the Fourth Assessment Report of the Intergovernmental Panel on

516 Climate Change, edited by S. Solomon *et al.*, pp. 591–662, Cambridge Univ. Press, Cambridge, U.K.

- 517 Ren, G.; Chu, Z.; Chen, Z.; Ren, Y. 2007 Implications of temporal change in urban heat island intensity observed at  
518 Beijing and Wuhan stations. *Geophys. Res. Lett.* , 34, L05711,doi:10.1029/2006GL027927.
- 519 Ren, G.-Y., Z.-Y. Chu, J.-X. Zhou, et al., (2008): Urbanization effects on observed surface air temperature in North  
520 China. *J. Climate*, 21, 1333-1348
- 521 Schmidt G. A. 2009 Spurious correlations between recent warming and indices of local economic activity, *Int. J. of*  
522 *Climatology*
- 523 Schneider,A., M. Friedl, and D. Potere, 2009:A new map of global urban extent from MODIS satellite data.  
524 *Environmental Research Letters*, 4(4), 044003, doi:10.1088/1748-9326/4/4/044003
- 525 Satterthwaite D.E., F. Aragón-Durand, J. Corfee-Morlot, R.B.R. Kiunsi, M. Pelling, D.C. Roberts, and W. Solecki,  
526 2014: Urban areas. In: *Climate Change 2014: Impacts, Adaptation, and Vulnerability. Part A: Global and*  
527 *Sectoral Aspects. Contribution of Working Group II to the Fifth Assessment Report of the Intergovernmental*  
528 *Panel on Climate Change (IPCC)*
- 529 Sciencing (2018) <https://sciencing.com/sun-intensity-vs-angle-23529.html>
- 530 Stone B. 2009 Land use as climate change mitigation, *Environ. Sci. Technol.*, 43( 24), 9052– 9056,  
531 doi:10.1021/es902150g
- 532 Sugawara, H., Takamura, T. Surface Albedo in Cities (0.12): Case Study in Sapporo and Tokyo, Japan. *Boundary-*  
533 *Layer Meteorol* **153**, 539–553 (2014). <https://doi.org/10.1007/s10546-014-9952-0>
- 534 US Population Growth 1900-2006, [u-s-history.com/pages/h980.html](http://u-s-history.com/pages/h980.html)
- 535 USGS 1900-2006, Materials in Use in U.S. Interstate Highways, <https://pubs.usgs.gov/fs/2006/3127/2006-3127.pdf>
- 536 USGS on Amount of Earth covered by water, [https://www.usgs.gov/special-topic/water-science-](https://www.usgs.gov/special-topic/water-science-school/science/how-much-water-there-earth?qt-science_center_objects=0#qt-science_center_objects)  
537 [school/science/how-much-water-there-earth?qt-science\\_center\\_objects=0#qt-science\\_center\\_objects](https://www.usgs.gov/special-topic/water-science-school/science/how-much-water-there-earth?qt-science_center_objects=0#qt-science_center_objects)
- 538 van Nes E. H., Scheffer M., Brovkin V., Lenton T. M., Ye H, Deyle E. and Sugihara G., *Nature Climate Change*  
539 2015. [dx.doi.org/10.1038/nclimate2568](https://doi.org/10.1038/nclimate2568)
- 540 World Bank, 2018 population growth rate, [worldbank.org](http://worldbank.org)
- 541 Yang, X.; Hou, Y.; Chen, B. 2011 Observed surface warming induced by urbanization in east China. *J. Geophys.*  
542 *Res. Atmos*, 116, doi:10.1029/2010JD015452.
- 543 Zhang, X., Friedl, M. A., Schaaf, C. B., Strahler, A. H. & Schneider, A. 2004 The footprint of urban climates on  
544 vegetation phenology. *Geophys. Res. Lett.* 31, L12209
- 545 Zhao, Z.-C., 1991: Temperature change in China for the last 39 years and urban effects. *Meteorological Monthly* (in  
546 Chinese), 17(4), 14-17.
- 547 Zhao, Z.-C., 2011: Impacts of urbanization on climate change. in: 10,000 Scientific Difficult Problems: Earth  
548 Science, 10,000 scientific difficult problems Earth Science Committee Eds., Science Press, 843-846. 30%
- 549 Zhao L, Lee X, Smith RB, Oleson K, Strong 2014, contributions of local background climate to urban heat islands,  
550 *Nature*. 10;511(7508):216-9. doi: 10.1038/nature13462
- 551 Zhou D. , Zhao S. , L. Zhang, G Sun and Y. Liu, 2015, The footprint of urban heat island effect in China, *Scientific*  
552 *Reports*. 5: 11160
- 553 Zhou Y. , SmithS. , Zhao K. , M. Imhoff, A. Thomson, B. Lamberty,G. Asrar, X. Zhang, C. He and C. Elvidge, A  
554 global map of urban extent from nightlights, *Env. Research Letters*, 10 (2015), (study uses a 2000 data set).

555  
556

557

**558 Conflicts of Interest**

559 The author declares that he has no conflicts of interest.

560